Microstructure and magnetic anisotropy of electrospun $Cu_{1-x}Zn_xFe_2O_4$ nanofibres: a local probe study

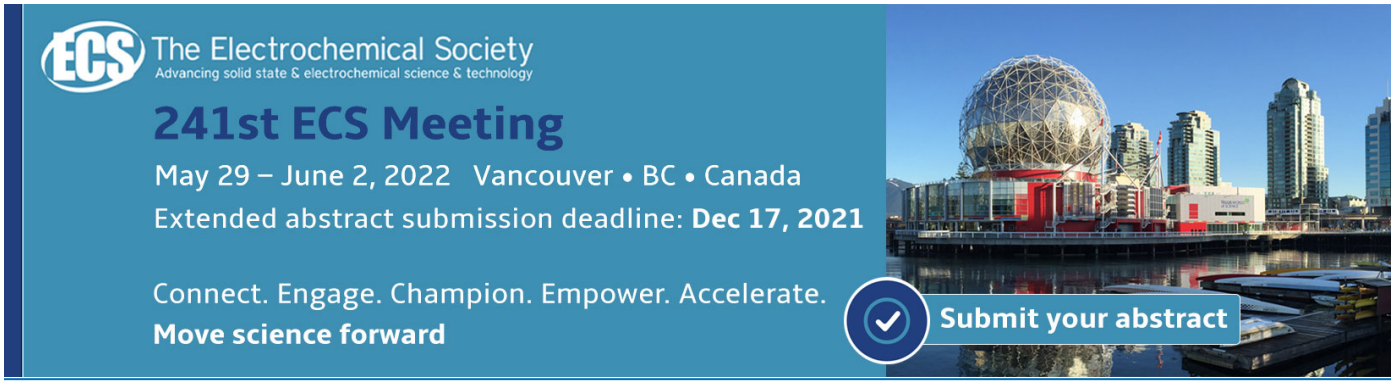

IOP PUBLISHING JOURNAL OF PHYSICS D: APPLIED PHYSICS

J. Phys. D: Appl. Phys. **44** (2011) 445304 (5pp) doi:10.1088/0022-3727/44/44/445304

Microstructure and magnetic anisotropy of electrospun $Cu_{1-x}Zn_xFe_2O_4$ nanofibres: a local probe study

Zhiwei Li[1], Weiwei Pan, Junli Zhang and Haibo Yi

Institute of Applied Magnetics, Key Lab for Magnetism and Magnetic Materials of the Ministry of Education, Lanzhou University, Lanzhou 730000, Gansu, People's Republic of China

E-mail: z.w.lee@live.cn

Received 15 July 2011, in final form 17 September 2011
Published 19 October 2011
Online at stacks.iop.org/JPhysD/44/445304

Abstract

Understanding phenomena at the nanometre scale is of fundamental importance for future improvements of desired properties of nanomaterials. We report a detailed investigation of the microstructure and the resulting magnetic anisotropy by magnetic, transmission electron microscopy (TEM) and Mössbauer measurements of electrospun $Cu_{1-x}Zn_xFe_2O_4$ nanofibres. Our results show that the electrospun $Cu_{1-x}Zn_xFe_2O_4$ nanofibres exhibit nearly isotropic magnetic anisotropy. TEM measurements indicate that the nanofibres are composed of loosely connected and randomly aligned nanograins. As revealed by the Henkel plot, these nanofibres and the nanograins within the nanofibres are dipolar coupled, which reduces the effective shape anisotropy leading to a nearly random configuration of the magnetic moments inside the nanofibres; hence, the observed nearly isotropic magnetic anisotropy can be easily understood.

(Some figures may appear in colour only in the online journal)

1. Introduction

Nanostructured materials find potential applications in many fields such as ultrahigh-density data storage, sensors, drug delivery systems and high-frequency devices [1–4] due to their distinctive properties that are not realized by their bulk counterparts. In particular, one-dimensional nanowires or nanofibres (NWFs) [1, 5–7] have recently received considerable interest not only because of their potential use but also because of their fundamental importance from a theoretical point of view [8, 9]. Among various preparation methods, electrospinning has proved to be an efficient process that can fabricate polymer NWFs on an industrial scale [10, 11]. And, over the last decade, remarkable progress has been made in applying this technique to the fabrication of magnetic NWFs [12].

Spinel ferrite NWFs are always an important subject of many research groups. And over the past few years, $TMFe_2O_4$ (TM = Ni, Co, Mg, Mn, etc) ferrite nanofibres have been synthesized using electrospinning and their magnetic properties have also been investigated in detail [13–16]. Copper ferrite is also an interesting material that has been widely used in many areas [17, 18]. In our previous work, $Cu_{1-x}Zn_xFe_2O_4$ nanofibres were prepared using the electrospinning technique and the influence of Zn^{2+} substitution on crystal structure, morphology and magnetic properties was investigated [19]. Usually, if the shape anisotropy dominates over the magnetocrystalline anisotropy, the easy magnetization direction should be along the long axis of a NFW [20]. Interestingly, however, we have found that the magnetic easy axis is not along the long axis of the nanofibres in sharp contrast to the usual observation.

In this study, in order to get a better understanding of the unusual magnetic anisotropy of the $Cu_{1-x}Zn_xFe_2O_4$ nanofibres, the microstructure of these nanofibres was studied in detail by transmission electron microscopy (TEM) and Mössbauer spectroscopy. The magnetic interactions of the sample were also investigated using the Henkel plot. The present results reveal dipolar interactions of our nanofibres, which reduce the effective shape anisotropy and explain well the observed unusual magnetic anisotropy.

2. Experiments

$Cu_{1-x}Zn_xFe_2O_4$ ($x = 0$–1.0) nanofibres were synthesized by electrospinning combined with the sol–gel technique [12, 19]. Phase purity was checked by x-ray diffraction (XRD) measurement using a Philips X'pert diffractometer with Cu K_α radiation. Morphology examination and elemental analysis were performed using a transmission electron microscope (TEM, FEI Tecnai F30) and a field emission scanning electron microscope (SEM, Hitachi S-480) equipped with an energy-dispersive x-ray spectrometer (EDXS). The dc magnetic properties were characterized using a vibrating sample magnetometer (VSM, Lakeshore 7403, USA). We will describe the details of sample preparation, structural and static magnetic properties elsewhere [19]. Transmission Mössbauer spectra (MS) were recorded at room temperature using a conventional constant acceleration spectrometer with a γ-ray source of 25 mCi ^{57}Co in a palladium matrix. The isomer shifts quoted in this work are relative to that of α-Fe.

For the dc magnetic and Mössbauer characterization, ~30 mg of the sample were weighed and then uniformly deposited on a thin nonmagnetic underlayer. From the SEM and TEM results we know that the nanofibres have a very large length-to-diameter ratio. So, the nanofibres should lie parallel to the sample plane during the measurements as illustrated in figure 1. In this case, the incident γ-rays should be perpendicular to the long axis of the nanofibres (figure 1(*a*)). For dc magnetic measurements, two different hysteresis loops were recorded with the magnetic field, H, applied in the y-axis direction (H should be parallel to the sample plane) and with H applied in the z-axis direction (H should be perpendicular to the sample plane), respectively.

3. Results and discussion

In figure 2, we present the hysteresis loops of $Cu_{0.6}Zn_{0.4}Fe_2O_4$ nanofibres. The lower inset is an enlargement of the low-field part of the magnetization curve. As described in the experimental section, parallel and perpendicular indicates that the hysteresis loops were measured with the magnetic field applied parallel and perpendicular to the sample plane, respectively. Usually, if the shape anisotropy dominates over the intrinsic magnetocrystalline anisotropy, an easy magnetization axis along the long axis of a nanowire is expected [20]. For the $Cu_{0.6}Zn_{0.4}Fe_2O_4$ nanofibres, the saturation magnetization is measured to be $M_S = 58.4\,\mathrm{emu\,g^{-1}}$, leading to an expected shape anisotropy of $K_{shape} = 3.2 \times 10^5\,\mathrm{erg\,cm^{-3}}$, which is much larger than the magnetocrystalline anisotropy for bulk copper ferrites, $\sim 0.6 \times 10^5\,\mathrm{erg\,cm^{-3}}$ [21]. This means that the expected easy axis should be along the nanofibres. Interestingly, one can see that the two hysteresis loops almost overlap. The same behaviour of the hysteresis loops was also found for other compositions, suggesting that the electrospun $Cu_{1-x}Zn_xFe_2O_4$ nanofibres have a smaller shape anisotropy than expected.

To examine the anisotropy more clearly, we now estimate the effective anisotropy field and compare it with experiments quantitatively. As is well known, the experimentally measured shape anisotropy field for nanowires can be expressed as $H_d = -NM_S$, where $N = 1/2$ is the demagnetization factor and M_S is the saturation magnetization. In our case, however, the experimentally measured effective anisotropy field, H_{eff}, should be different since the nanofibres are randomly aligned within the sample plane. In order to calculate H_{eff}, we first deduce the effective demagnetization factor for a disc-like sample composed of randomly aligned nanofibres. We define θ to be the angle between the applied magnetic field and the long axis of a nanofibre (figure 1(*b*)). Then, the demagnetization energy can be expressed as [9]

$$E_d = \tfrac{1}{2}\mu_0 N_\theta M^2 = \tfrac{1}{2}\mu_0 (N_\parallel M_\parallel^2 + N_\perp M_\perp^2) = \tfrac{1}{2}\mu_0 N_\perp (M_S \sin\theta)^2, \quad (1)$$

where $\parallel$ / $\perp$ indicates parallel/perpendicular to the long axis of the nanofibre. Rewriting equation (1) as $E_d = \frac{1}{2}\mu_0 (N_\perp \sin^2\theta) M_S^2$, one could get the demagnetization factor for a nanofibre along the θ direction, $N_\theta = N_\perp \sin^2\theta = \frac{1}{2}\sin^2\theta$. For a disc-like sample composed of uniformly aligned nanofibres, the effective demagnetization factor can be determined to be $N_{eff} = 1/4$ by integrating N_θ over all possible directions. Then, the effective anisotropy field is expressed as

$$H_{eff} = |-N_\perp M_S - (-N_{eff} M_S)| = \tfrac{1}{4} M_S. \quad (2)$$

Using the measured $M_S = 58.4\,\mathrm{emu\,g^{-1}}$, we can calculate the effective anisotropy field to be $H_{eff} = 1006\,\mathrm{Oe}$. This value is much larger than the measured value from the hysteresis loops, $H_k \sim 600\,\mathrm{Oe}$, which is deduced as twice that of the shaded area [22] indicated in the lower inset of figure 2. This suggests that the effective anisotropy is rather different from that expected for nanowires that are dominated by the shape anisotropy. In other words, if we consider one single nanofibre, the easy magnetization direction is not along the long axis of the fibre, which is evidenced by our Mössbauer measurements. Different magnetic anisotropy was also observed by Pullar and Bhattacharya [23] in randomly oriented M hexa-ferrite fibres, where they showed that alignment effects play important roles in deciding the anisotropy effect.

To understand the above observed unusual anisotropy effect, Mössbauer measurements were employed to probe the microscopic spatial distribution of the magnetic moments inside the nanofibres. Figure 3 shows the room temperature ^{57}Fe Mössbauer spectra of the $Cu_{1-x}Zn_xFe_2O_4$ ($x = 0$–1.0) nanofibres. The fitted hyperfine parameters are given in table 1. Clearly, the spectrum evolves from two sextets (corresponding to the Fe atoms sitting at tetrahedral (A) sites and octahedral (B) sites, respectively) for $x = 0$ to a quadrupole split doublet for $x = 0.6$, indicating the collapse of the long-range magnetic order upon Zn substitution, coincident with magnetization measurements [19]. From the shape of the spectra one can see that the sextets broaden, instead of the superposition of the sextets and the doublet, as x increases till the collapse point for $x = 0.6$, which is an indication of homogeneous Zn substitution of Cu ions.

To exclude the spectral line broadening effect on the relative intensity ratio of the six lines, we take $CuFe_2O_4$ as an example to investigate the microscopic spatial distribution

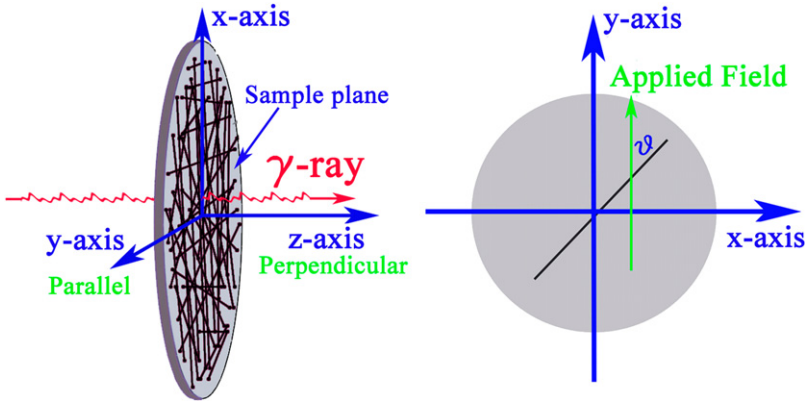

Figure 1. Schematic diagram for the dc magnetic and Mössbauer measurements (left) and front view of the sample plane (right) (see the text).

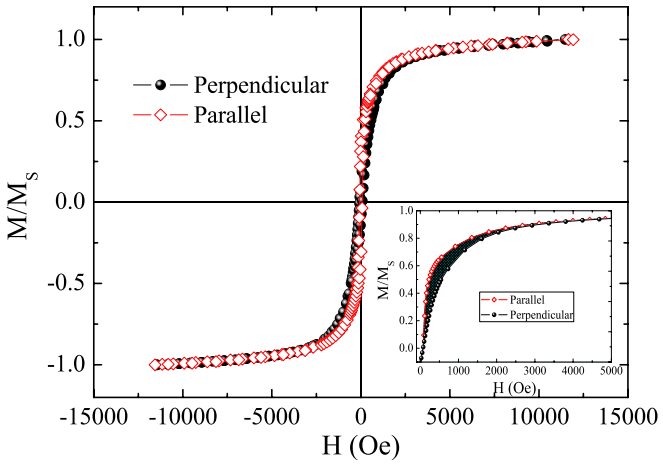

Figure 2. Typical hysteresis loops of $Cu_{0.6}Zn_{0.4}Fe_2O_4$ nanofibres. The measurements were done with the magnetic field applied parallel (red open diamonds) and perpendicular (black solid circles) to the sample plane, respectively. The right-lower inset is an enlargement of the low-field part of the magnetization curve and the shaded area indicates the difference between the two curves.

of the magnetic moments inside the nanofibres. In Mössbauer measurements, as is well known, the direction of the magnetic moments can be deduced by the relative intensities of the six absorption lines of the Zeeman split sextet. The relative intensities as a function of the polar angle θ between the magnetic moment and the incident γ-rays is expressed as [24]

$$\frac{I_{2,5}}{I_{1,6}} = \frac{4\sin^2\theta}{3(1+\cos^2\theta)}, \tag{3}$$

where $I_{2,5}$ and $I_{1,6}$ are the line intensities of the 2,5th and 1,6th peaks of the magnetically split sextet, respectively. The best fit of our Mössbauer spectra for $CuFe_2O_4$ yields $I_{2,5}/I_{1,6} = 2.25$, which is close to the value of 2 for samples with randomly aligned magnetic moments. This is in sharp contrast to the usual expected value of 4 for nanowires where the magnetic moments usually align parallel to the long axis of the nanowires due to the shape anisotropy. This result explains well why the measured effective anisotropy is much smaller than expected.

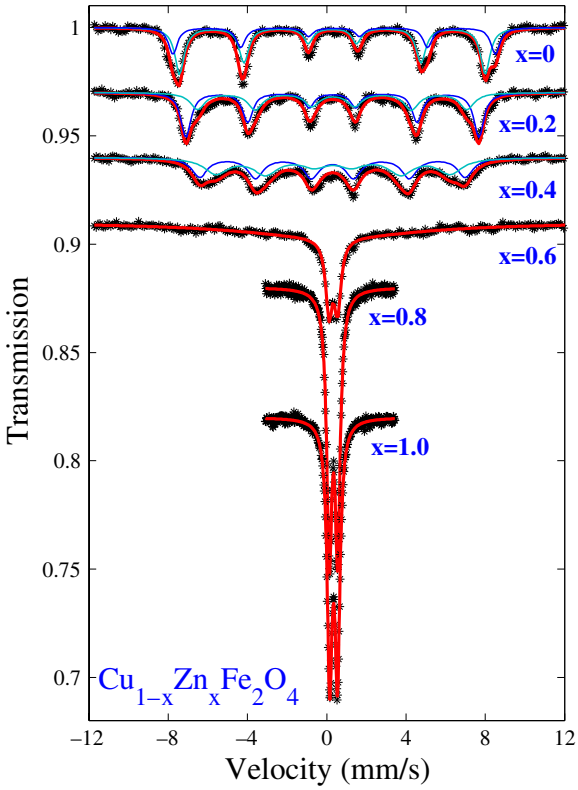

Figure 3. Mössbauer spectra of the $Cu_{1-x}Zn_xFe_2O_4$ ($x = 0$–1.0) nanofibres taken at room temperature. The spectra were fitted with two sextets for $x = 0$, 0.2 and 0.4 and with only one doublet for $x = 0.8$ and 1.0.

TEM was employed to further examine the microstructures of the $CuFe_2O_4$ nanofibres. In figures 4(*a*)–(*c*), we present the TEM micrographs of the nanofibres, from which one can see that the nanofibres are about ∼200 nm in diameter. A closer look at the nanofibres reveals that these fibres are composed of smaller grains of about ∼50 nm size and are loosely connected with each other. Crystalline lattice structures are clearly shown in the high magnification TEM images, figures 4(*b*) and (*c*), indicating good crystallinity of our sample. Figure 4(*f*) shows the selected area electron diffraction (SAED) pattern of a single fibre. All the bright

rings can be indexed to the cubic spinel structure. Another important fact one can infer from the bright rings of the SAED pattern is that the small grains are randomly oriented in the fibre.

As we know, the NWFs are usually composed of closely connected smaller grains, ~several nanometres. And according to Herzer's statement [25], when the grain size (D) along with the intergranular distance (S) is smaller than the exchange length ($L_{ex} = \sqrt{2A/(\mu_0 M_S^2)}$), exchange coupling takes place. The magnetocrystalline anisotropy will be suppressed by the exchange coupling, $\langle K \rangle = K_1/\sqrt{N}$, where K_1 is the magnetocrystalline anisotropy constant and N is the granular amount within the volume of $V = L_{ex}^3$. This will effectively increase the demagnetization effect, which favours the fact that the magnetization aligns parallel to the long axis of the nanowires. If we adopt the value of $A = 1.2 \times 10^{-11}\,\mathrm{J\,m^{-1}}$ [26], the estimated exchange length is $L_{ex} \sim 33.8\,\mathrm{nm}$. In the present nanofibres, as learned from TEM results, the size of the small grains (~50 nm) exceeds this characteristic length. Thus, dipolar interaction should be expected in the present $Cu_{1-x}Zn_xFe_2O_4$ nanofibres, which means that the magnetization in two neighbouring grains favour an antiparallel alignment.

Table 1. Hyperfine parameters of $Cu_{1-x}Zn_xFe_2O_4$ ($x = 0$–1.0) nanofibres extracted from least-squares fit of the Mössbauer spectra shown in figure 3. δ denotes the isomer shift, ΔE_Q is the quadrupole splitting and B_{hf} is the hyperfine magnetic field.

Sample	Site	δ (mm s^{-1})	ΔE_Q (mm s^{-1})	B_{hf} (T)
$x = 0.0$	A	0.281(10)	−0.024(10)	47.97(11)
	B	0.365(17)	−0.012(17)	50.86(16)
$x = 0.2$	A	0.288(12)	−0.001(12)	45.82(12)
	B	0.305(29)	−0.025(29)	42.15(45)
$x = 0.4$	A	0.288(22)	−0.012(22)	41.44(34)
	B	0.325(45)	−0.032(41)	36.29(81)
$x = 0.6$	—	0.335(10)	0.439(14)	—
$x = 0.8$	—	0.342(2)	0.416(4)	—
$x = 1.0$	—	0.346(2)	0.393(3)	—

To prove our above arguments, we further study the magnetic interactions of the small grains inside the nanofibres. A useful tool for studying the interactions among magnetic nanograins is the Henkel plot or the $\delta m(H)$ plot [27, 28]. It is well known, for an assembly of magnetically noninteracting nanograins, that the isothermal remanent magnetization $M_r(H)$ and the dc demagnetization remanence $M_d(H)$ should obey the Stoner–Wohlfarth relation:

$$M_d(H) = M_r(\infty) - 2M_r(H), \tag{4}$$

where $M_r(\infty)$ is the maximum remanent magnetization measured after saturation. Henkel first proposed that the deviation of the measured $M_d(H)$ and $M_r(\infty) - 2M_r(H)$ can be used to study the magnetic interactions in real systems. The Henkel plot is expressed as follows [27]:

$$\delta m(H) = \frac{M_d(H) - (M_r(\infty) - 2M_r(H))}{M_r(\infty)}. \tag{5}$$

Positive values of $\delta m(H)$ are due to exchange interactions promoting the magnetized state, while negative values of $\delta m(H)$ correspond to dipolar interactions tending to assist magnetization reversal.

Typical room temperature $\delta m(H)$ plot for $CuFe_2O_4$ nanofibres is shown in figure 5. As can be seen, two minimum values of the $\delta m(H)$ curve, possibly due to inter-fibre and inter-grain interactions, are observed [29–31]. Negative values of $\delta m(H)$ are indicative of a dipolar type of interaction, which is

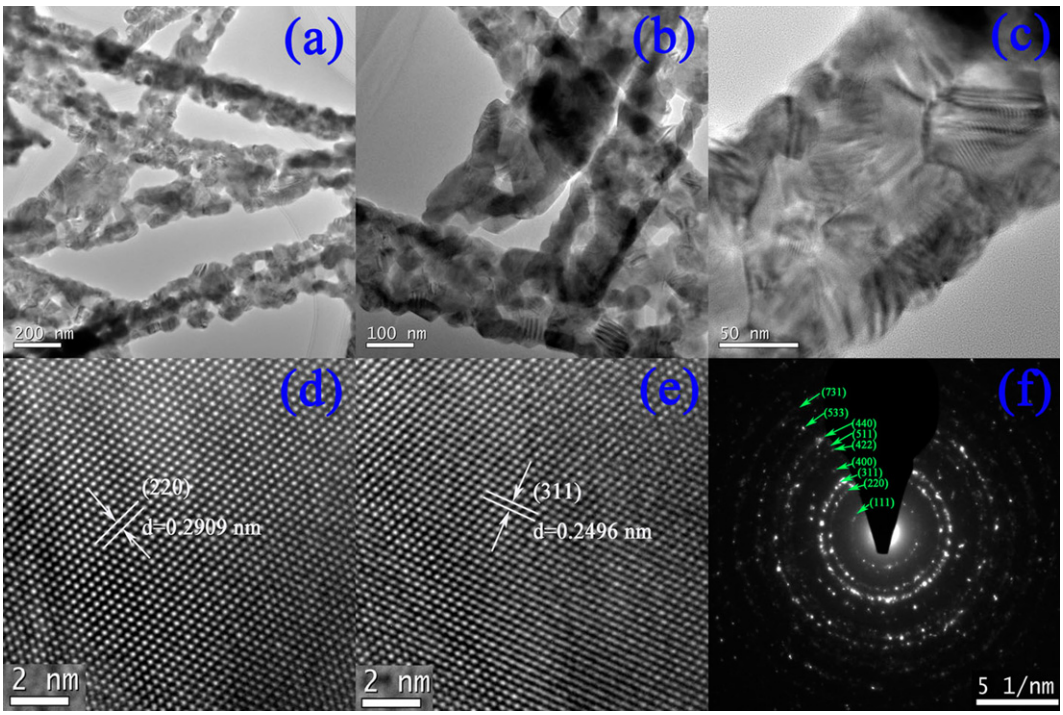

Figure 4. TEM micrographs of the $CuFe_2O_4$ nanofibres (a)–(c), high magnification TEM images of the nanofibres showing the crystalline lattice structures (d), (e), and the corresponding SAED pattern of a single fibre (f).

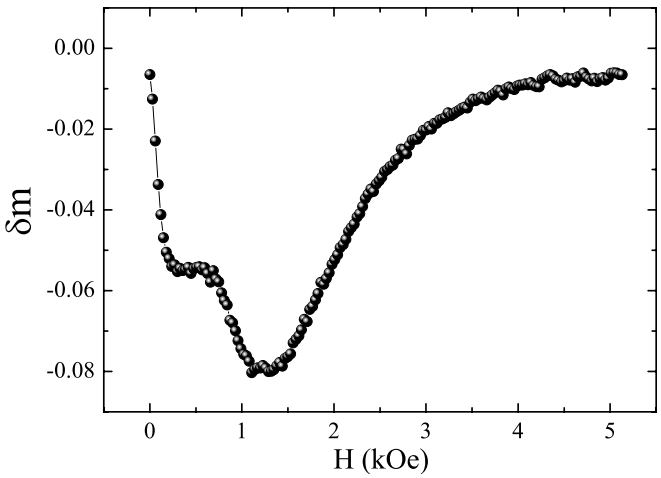

Figure 5. $\delta m(H)$ plot of the $CuFe_2O_4$ nanofibres.

expected in the case of loosely connected nanograins. Thus, we can conclude that the present nanofibres are composed of dipolar coupled nanograins and the interaction between these nanofibres is also of dipolar type, which tend to assist the magnetization reversal process, hence reducing the effective shape anisotropy and leading to the above observed unusual magnetic anisotropy effect.

4. Concluding remarks

In summary, we have studied the microstructure and magnetic anisotropy effect of electrospun $Cu_{1-x}Zn_xFe_2O_4$ nanofibres. Magnetic and Mössbauer measurements reveal that the electrospun nanofibres have a rather isotropic magnetic anisotropy. This is in sharp contrast to the usual case for nanowires prepared by conventional methods. From the negative values of the $\delta m(H)$ plot as well as the TEM results, we can conclude that the present nanofibres are composed of randomly aligned and dipolar coupled nanograins, and these nanofibres are also dipolar coupled, which reduces the effective shape anisotropy and explains well the observed unusual magnetic anisotropy effect.

Acknowledgments

The author (Li Zhiwei) is grateful to Dr X Yang for useful discussions. This work was supported by the National Natural Science Foundation of China under Grant No 10774061.

References

[1] Xia Y N *et al* 2003 *Adv. Mater.* **15** 353
[2] Neuberger T *et al* 2005 *J. Magn. Magn. Mater.* **293** 483
[3] Sawhney A P S *et al* 2008 *Textile Res. J.* **78** 731
[4] Kou X *et al* 2009 *Appl. Phys. Lett.* **94** 112509
[5] Baji A *et al* 2011 *Nanotechnology* **22** 235702
[6] Chen S F *et al* 2010 *Nanotechnology* **21** 425602
[7] Zhang T *et al* 2005 *Nanotechnology* **16** 2743
[8] Moon K W *et al* 2009 *Curr. Appl. Phys.* **9** 1293
[9] Bergmann G *et al* 2008 *Phys. Rev.* B **77** 054415
[10] Bhardwaj N *et al* 2010 *Biotechnol. Adv.* **28** 325
[11] Feng C *et al* 2010 *J. Appl. Polym. Sci.* **115** 756
[12] Ramaseshan R *et al* 2007 *J. Appl. Phys.* **102** 111101
[13] Li D *et al* 2003 *Appl. Phys. Lett.* **83** 4586
[14] Sangmanee M *et al* 2009 *Appl. Phys.* A **97** 167
[15] Maensiri S *et al* 2009 *Nanoscale Res. Lett.* **4** 221
[16] Xiang J *et al* 2009 *Mater. Chem. Phys.* **114** 362
[17] Tao S W *et al* 2000 *Mater. Sci. Eng.* **77** 172
[18] Tsoncheva T *et al* 2010 *Catal. Commun.* **12** 105
[19] Pan W W *et al* 2011 arXiv:1106.1269
[20] Huang Z B *et al* 2008 *J. Colloid Interface Sci.* **317** 530
[21] Buschow K H J (ed) 1995 *Handbook of Magnetic Materials* vol 8 (Amsterdam: North-Holland) p 212
[22] Neudert A *et al* 2004 *J. Appl. Phys.* **95** 6595
[23] Pullar R C *et al* 2006 *J. Magn. Magn. Mater.* **300** 490
[24] Gütlich P *et al* 2011 *Mössbauer Spectroscopy and Transition Metal Chemistry* (Berlin: Springer) p 113
[25] Herzer G *et al* 1990 *IEEE Trans. Magn.* **26** 1397
[26] Dantas C C *et al* 2010 *J. Magn. Magn. Mater.* **322** 2824
[27] Fodor P S *et al* 2008 *J. Appl. Phys.* **103** 07B713
[28] Yao D S *et al* 2008 *J. Appl. Phys.* **104** 013902
[29] Zighem F *et al* 2011 *J. Appl. Phys.* **109** 013910
[30] Zhan Q F *et al* 2005 *Phys. Rev.* B **72** 024428
[31] Malik R *et al* 2008 *J. Appl. Phys.* **104** 064317